Modifying Ventricular Fibrillation by Targeted Rotor Substrate Ablation: Proof-of-Concept from Experimental Studies to Clinical VF

Online Supplement

David E. Krummen, MD, FHRS[1,2]
Justin Hayase, MD[1,2]
Stephen P. Vampola, MD[1,2]
Gordon Ho, MD[1,2]
Amir A. Schricker, MD[1,2]
Gautam G. Lalani, MD[1,2]
Tina Baykaner, MD[1,2]
Taylor M. Coe, BS[3]
Paul Clopton, MS[2]
Wouter-Jan Rappel, PhD[4]
Jeffrey H. Omens, PhD[3]
Sanjiv M. Narayan, MD, PhD, FHRS[5]

[1]Dept. of Medicine, University of California San Diego
[2]Veterans Affairs San Diego Healthcare System, San Diego, CA
[3]Dept. of Bioengineering, University of California San Diego
[4]Dept. of Physics, University of California San Diego
[5]Stanford University, Palo Alto, CA

Table of Contents

I. Supplemental Movie Descriptions

Supplemental Movie 1: Movie shows a canine left ventricular rotor in a 20 kg animal with a VF cycle length of 127 msec. The rotor is initially observed in the mid-septal LV where it completes 11 counter-clockwise rotations, then precesses to the basal LV for 2 rotations, before returning to the mid-septal LV for 2 more rotations. The phase singularity for this rotor is identified by the pink dot (left center of movie). This episode of ventricular fibrillation was terminated with defibrillation. Video axes are similar to manuscript figure 2B: the LV base is at top and apex at bottom, anterior is on the left side and lateral is on the right side.

Supplemental Movie 2: Movie shows a human left ventricular rotor in the mid-lateral LV in a 68 year old male with an ejection fraction of 32% with clinical VF. The counterclockwise rotor (phase singularity at pink dot at upper right center of movie) has a cycle length of 213 msec and completes 10 rotations while precessing slightly apically and then laterally. This episode required defibrillation for termination. Video axes are similar to manuscript figure 5D: the LV base is at top and apex at bottom, anterior is on the left side and lateral is on the right side.

II. Data Supplement: Canine and Human Purkinje Analysis

Prior work has revealed that triggering PVCs for VF may originate from the Purkinje network in patients with idiopathic VF.[1] However, the relationship between Purkinje potentials and VF rotor substrate sites in patients with structural heart disease is unclear. To address this question, we quantified the proportion of VF substrate sites with potential Purkinje potentials in both the canine VF model and the human patient with clinical VF.

In canines, baseline bipolar basket electrograms were recorded in sinus rhythm. Using these recordings, we analyzed for Purkinje activity at rotor sites. Once rotors were identified using phase analysis,[2, 3] we localized the rotor core (phase singularity) to the 4 bounding electrode pairs. We then analyzed each electrogram for the presence of potential Purkinje potentials, as shown in figure S1A. The percentage of Purkinje activity represents the number of electrograms with potential Purkinje activity divided by the total number of electrograms analyzed.

In the human case, we analyzed bipolar electrograms recorded from the ablation catheter at each rotor substrate ablation lesion. The percent of Purkinje activity was calculated as the total number of unique ablation sites with potential Purkinje activity divided by the total number of unique ablation sites. An example human Purkinje potential is shown in figure S1B.

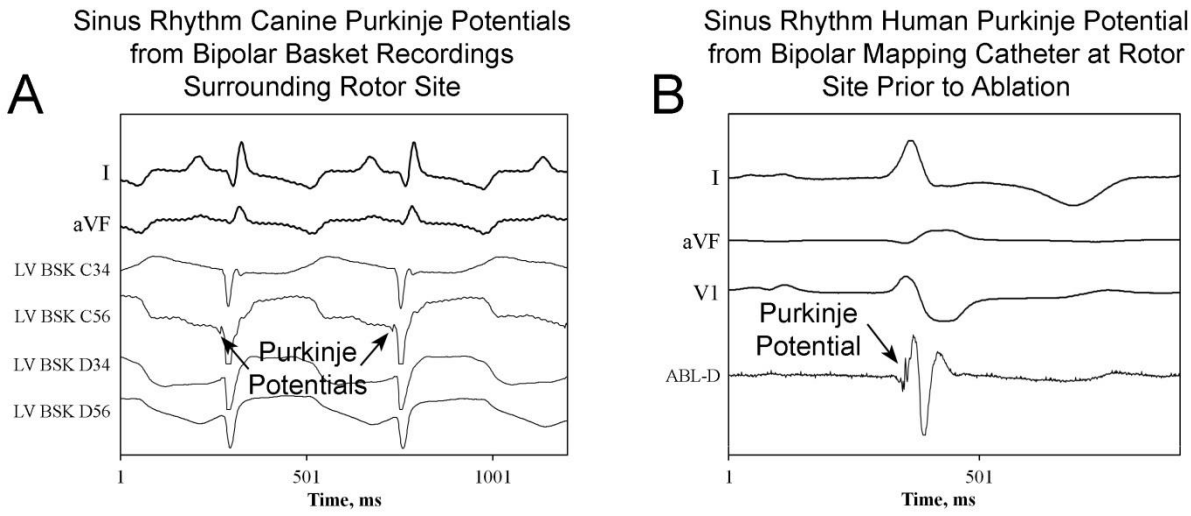

Figure S1. Canine and Human Purkinje Analysis. (A) Canine Purkinje potentials are seen on 1 of 4 LV basket electrograms (electrode pair C5-6) surrounding an identified rotor phase singularity. (B) Human Purkinje potentials were recorded from few sites prior to ablation on the ablation catheter distal electrode pair.

Overall, Purkinje potentials were rare, seen at a minority (9±14%) of canine rotor substrate electrograms and only 11% of human electrograms recorded from rotor substrate ablation sites, and not at LV rotor site 1 or RV rotor site 2. These findings are consistent with the hypothesis that rotor substrate sites are often distinct from Purkinje fibers and may arise from the papillary muscles[4] (canines) and diseased substrate sites[5, 6] (patient with structural heart disease). Future mapping studies are required to clarify the precise role of the Purkinje network during VF.

III. Data Supplement: Canine Sham and Rotor Substrate Ablation

Sham and rotor substrate site ablation were performed to evaluate their respective effects on VF inducibility. Sham ablation sites were selected at least 3 cm from rotor locations in the LV (n=4) or RV (n=5). Examples of each are shown in figure S2 (below).

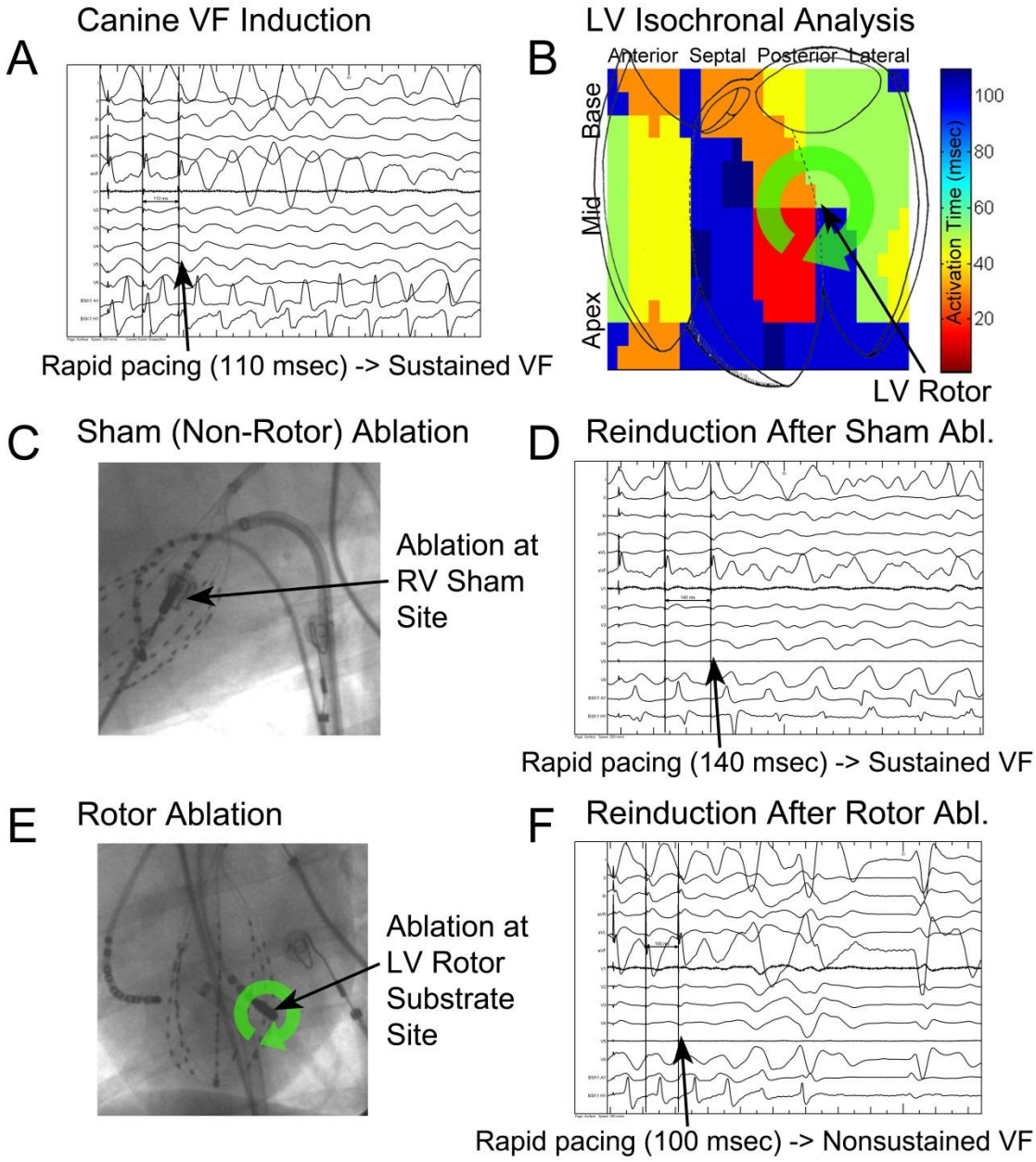

Figure S2. Canine Sham (Non-Rotor) and Rotor Substrate Ablation. (A) Rapid pacing at a CL of 110 msec induces sustained VF, requiring defibrillation. (B) Isochronal analysis illustrates a LV mid posterolateral rotor. (C) Left lateral cine showing ablation catheter and LV basket, with

sham ablation targeting the lateral RV where no rotors were observed; 6 minutes of RF were delivered to an area of 1.8 cm^2. (D) Following sham ablation, VF was induced with 5 seconds of rapid pacing at a CL of 140 msec. (E) Left anterior oblique cine showing ablation catheter and LV basket during ablation of the LV rotor substrate site. (F) Following rotor ablation, rapid pacing for 5 seconds at 110 msec does not induce sustained VF. Shorter pacing CLs produced 2:1 capture.

As discussed in the manuscript, sham ablation had no appreciable impact on VF inducibility, whether performed before or after rotor site ablation. An important corollary of this observation is that localized ablation (~2 cm^2) did not paradoxically create substrate promoting VF initiation and maintenance in canines, thus addressing a safety concern for translating this technique to patients.

IV. Data Supplement: Details of Pre-ablation ATP

Prior to the clinical VF rotor substrate ablation, we investigated 2 events seen on ICD interrogation which were classified as successful ATP therapy for VF (manuscript figure 6F). Details from ICD interrogation of these events are shown below (Figure S3).

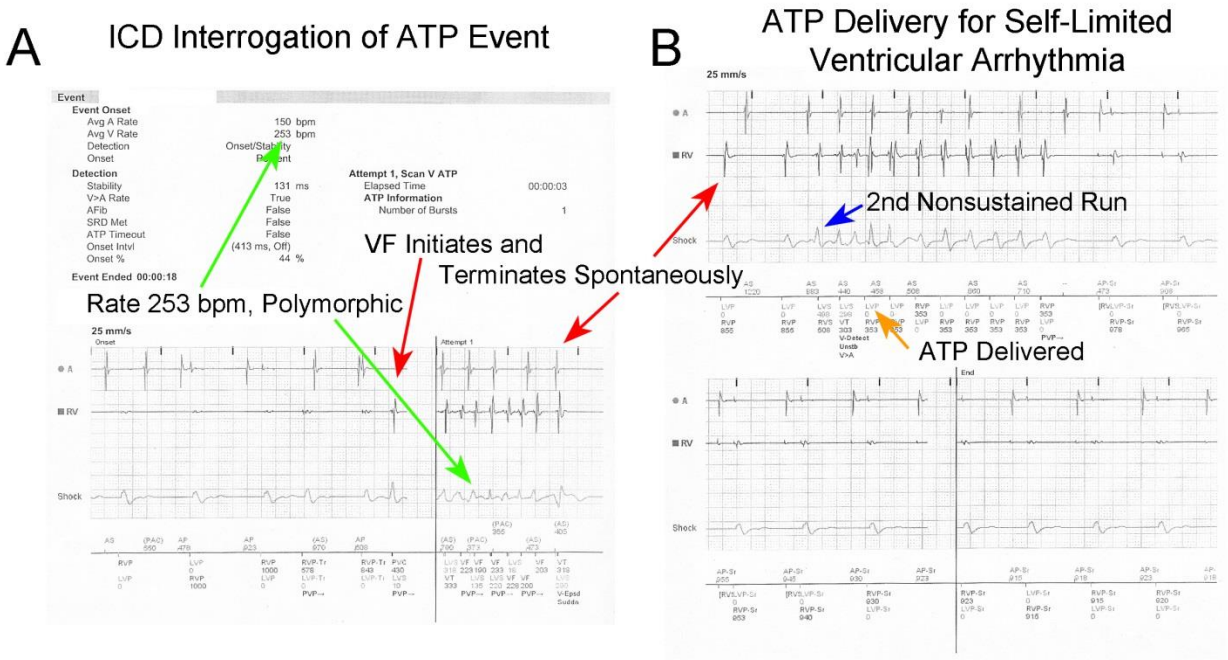

Figure S3. Pre-ablation ICD Interrogation of ATP Therapy. (A) Event is classified as a successful ATP for a ventricular arrhythmia in the VF zone (rate 253 bpm and with changing morphology, green arrows). However, electrogram analysis shows that VF initiates and spontaneously terminates (text and red arrows) prior to delivery of ATP. (B) A second instance of nonsustained arrhythmia is seen (blue arrow), which terminates prior to delivery of the 3rd ATP impulse (orange arrow at beginning of ATP).

ICD interrogation shows nonsustained VF which terminates prior to ATP (Figure S3A). As shown in Figure S3B, a second ventricular arrhythmia, beginning just prior to ATP therapy, terminates prior to the 3rd impulse of ATP, inconsistent with sustained VF,[7] and therefore this pre-ablation event represents ATP delivered to self-limited ventricular arrhythmias.

V. Data Supplement: References

1. Haissaguerre M, Shoda M, Jais P, Nogami A, Shah DC, Kautzner J, Arentz T, Kalushe D, Lamaison D, Griffith M, Cruz F, de Paola A, Gaita F, Hocini M, Garrigue S, Macle L, Weerasooriya R, Clementy J. Mapping and ablation of idiopathic ventricular fibrillation. *Circulation*. 2002;106:962-967.
2. Nash MP, Mourad A, Clayton RH, Sutton PM, Bradley CP, Hayward M, Paterson DJ, Taggart P. Evidence for multiple mechanisms in human ventricular fibrillation. *Circulation*. 2006;114:536-542.
3. Umapathy K, Nair K, Masse S, Krishnan S, Rogers J, Nash MP, Nanthakumar K. Phase mapping of cardiac fibrillation. *Circulation. Arrhythmia and electrophysiology*. 2010;3:105-114.
4. Kim YH, Xie F, Yashima M, Wu TJ, Valderrabano M, Lee MH, Ohara T, Voroshilovsky O, Doshi RN, Fishbein MC, Qu Z, Garfinkel A, Weiss JN, Karagueuzian HS, Chen PS. Role of papillary muscle in the generation and maintenance of reentry during ventricular tachycardia and fibrillation in isolated swine right ventricle. *Circulation*. 1999;100:1450-1459.
5. Masse S, Downar E, Chauhan V, Sevaptsidis E, Nanthakumar K. Ventricular fibrillation in myopathic human hearts: Mechanistic insights from in vivo global endocardial and epicardial mapping. *Am J Physiol Heart Circ Physiol*. 2007;292:H2589-2597.
6. Nair K, Umapathy K, Farid T, Masse S, Mueller E, Sivanandan RV, Poku K, Rao V, Nair V, Butany J, Ideker RE, Nanthakumar K. Intramural activation during early human ventricular fibrillation. *Circulation. Arrhythmia and electrophysiology*. 2011;4:692-703.
7. KenKnight BH, Bayly PV, Gerstle RJ, Rollins DL, Wolf PD, Smith WM, Ideker RE. Regional capture of fibrillating ventricular myocardium. Evidence of an excitable gap. *Circulation research*. 1995;77:849-855.